

Supporting Information

**Binding Modes and Pathway of RHPS4 to Telomeric G-Quadruplex and Duplex DNA
Probed by All-Atom Molecular Dynamics Simulations with Explicit Solvent**

by Kelly Mulholland, Farzana Siddiquei and Chun Wu

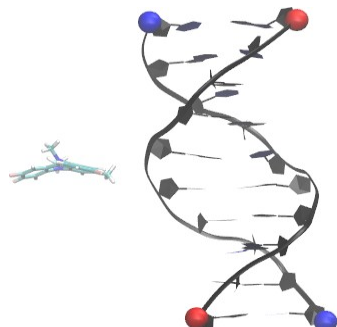
Table S1. Summary of RHPS4 use in treating various cancers

Cell line	Target	Disease	Reference
U251MG, U87MG, T67 and T70	Telomeric G-quadruplex	Astrocytoma	1
DAOY	Telomeric G-quadruplex	Medulloblastoma	2
PFSK-1 CNS PNET	Telomeric G-quadruplex	CNS primitive neuroectodermal	2
U87, KNS42	Telomeric G-quadruplex	Glioblastoma	2
Res196	Telomeric G-quadruplex	Ependymoma	2
C6	Telomeric G-quadruplex	Glioma	2
HCT116	Telomeric G-quadruplex	Colorectal	3

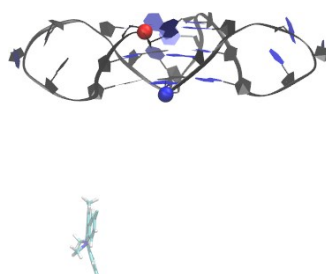
1. Berardinelli, F.; Siteni, S.; Tanzarella, C.; Stevens, M. F.; Sgura, A.; Antoccia, A., The G-quadruplex-stabilising agent RHPS4 induces telomeric dysfunction and enhances radiosensitivity in glioblastoma cells. *DNA Repair* **2015**, 25, 104-115
2. Lagah, S.; Tan, I. L.; Radhakrishnan, P.; Hirst, R. A.; Ward, J. H.; O'Callaghan, C.; Smith, S. J.; Stevens, M. F. G.; Grundy, R. G.; Rahman, R., RHPS4 G-Quadruplex Ligand Induces Anti-Proliferative Effects in Brain Tumor Cells. *Plos One* **2014**, 9
3. Johnson, L. A.; Byrne, H. M.; Willis, A. E.; Laughton, C. A., An integrative biological approach to the analysis of tissue culture data: application to the antitumour agent RHPS4. *Integrative Biology* **2011**, 3, 843-849

Figure S2. Initial structures of the simulation systems with unbound RHPS4: duplex DNA (A), parallel quadruplex DNA (B, pdb 1KF1), antiparallel DNA quadruplex (C, pdb 143D) and hybrid DNA quadruplex (D, 2HY9). 5' and 3' are indicated by a red and blue ball, respectively.

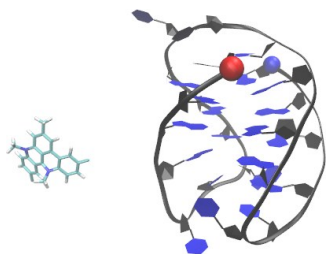
A)



B)



C)



D)

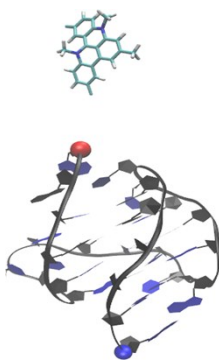


Figure S3. RMSD plot of each system: 1NZM (with complex, ligand alone and receptor alone in red, green and blue, respectively) (A), duplex DNA (B), parallel quadruplex DNA (C), anti-parallel quadruplex DNA (D), and hybrid quadruplex DNA (E).

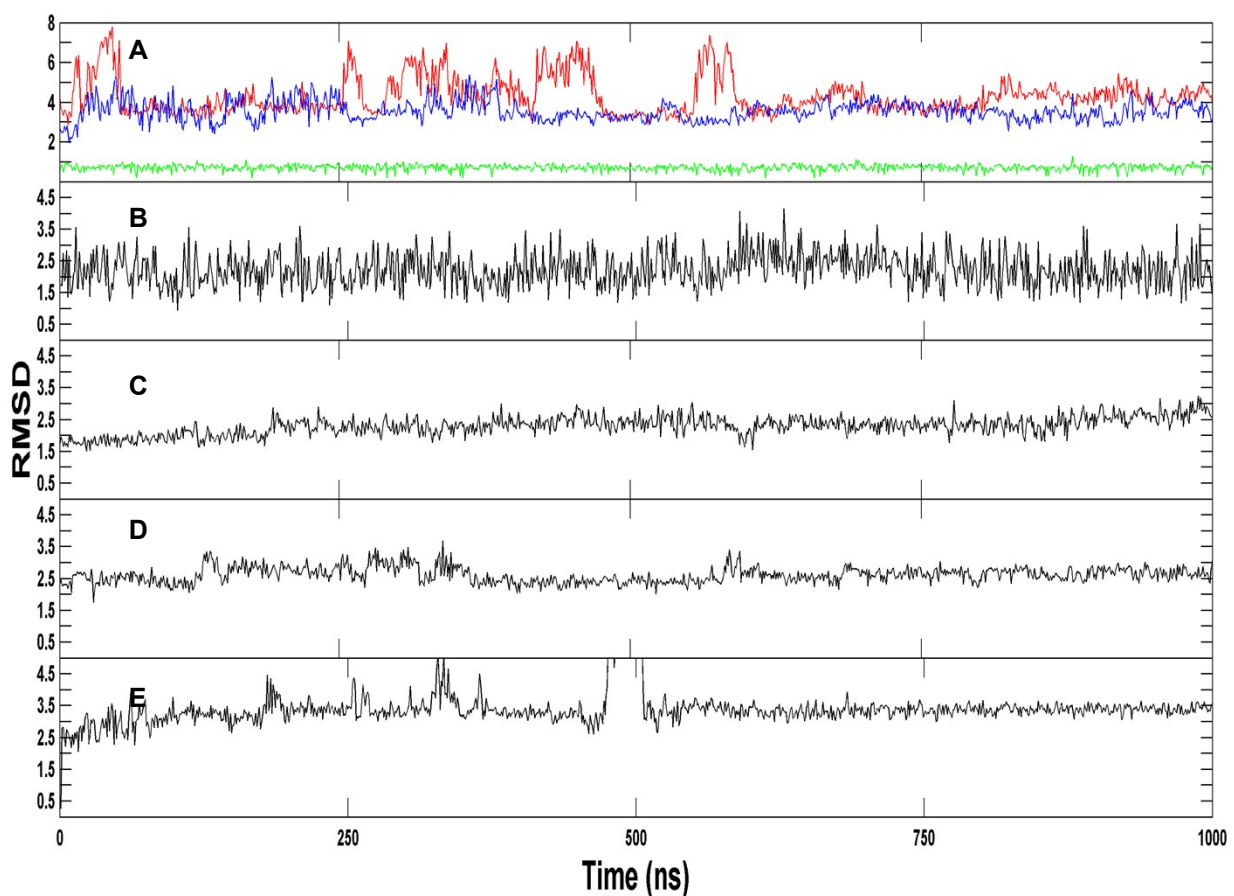


Figure S4. RMSD of duplex DNA system and RHPs4 of each trajectory

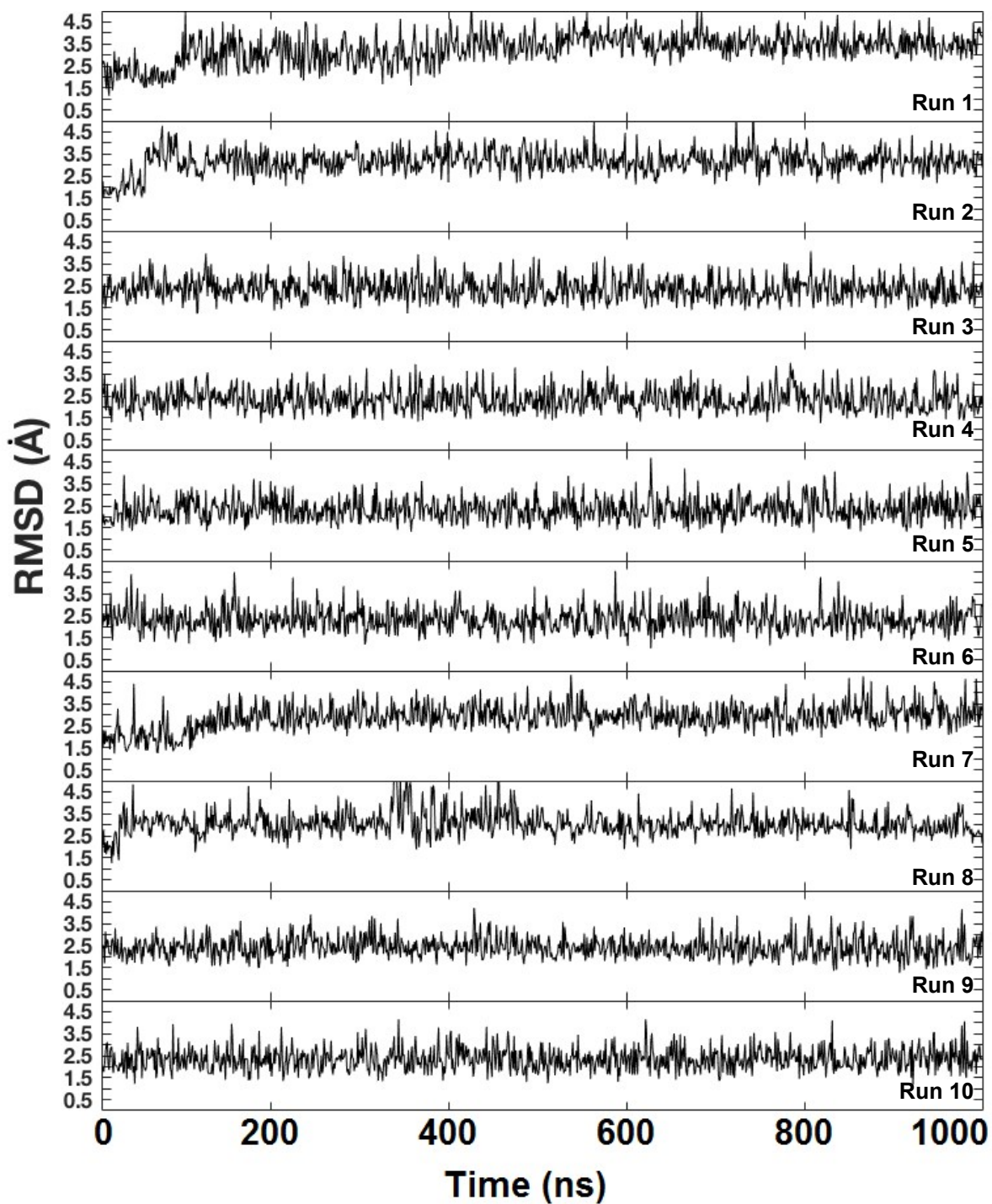


Figure S5. RMSD of parallel DNA quadruplex system and RHPs4 of each trajectory

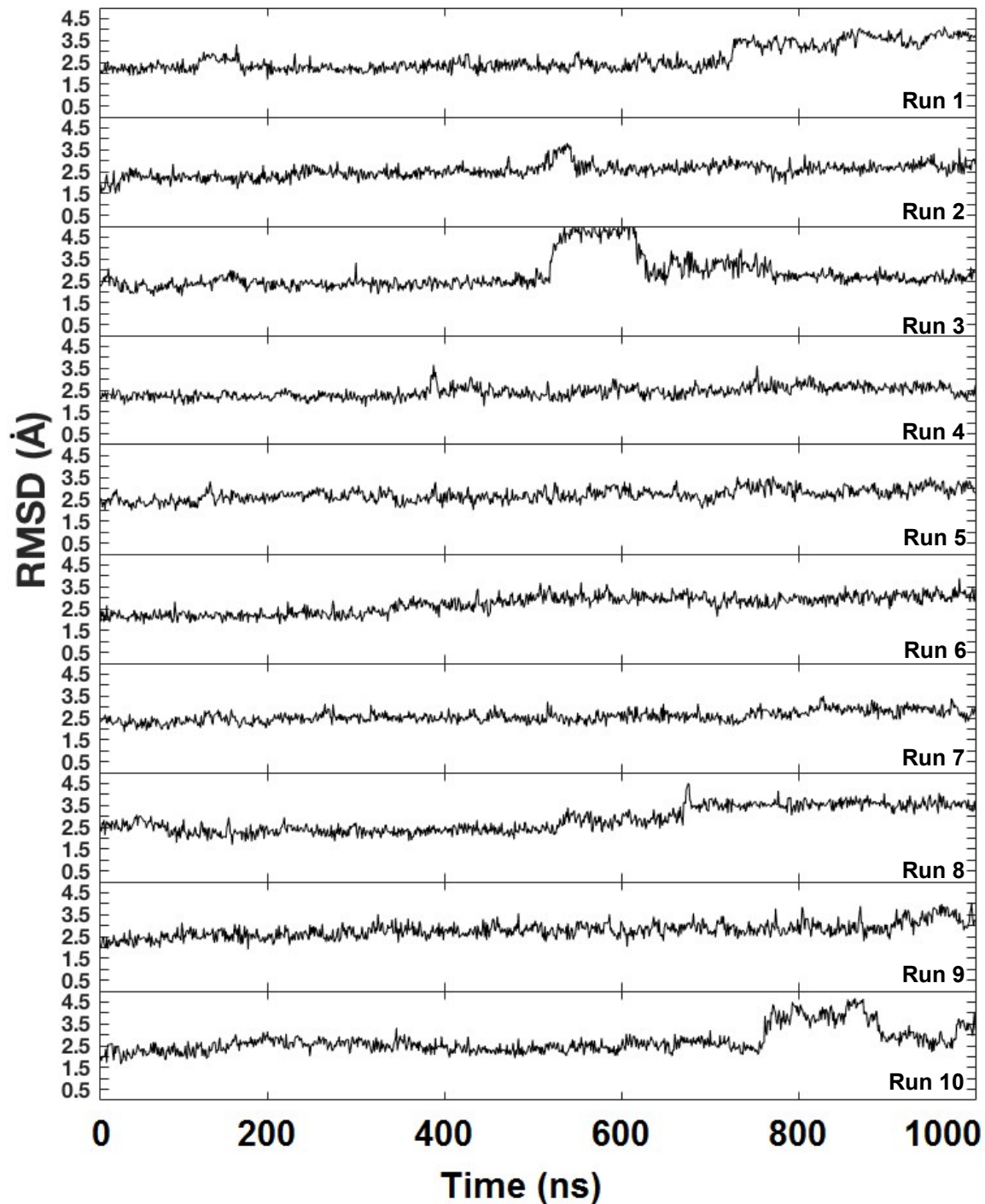


Figure S6. RMSD of antiparallel DNA quadruplex system and RHPS4 of each trajectory

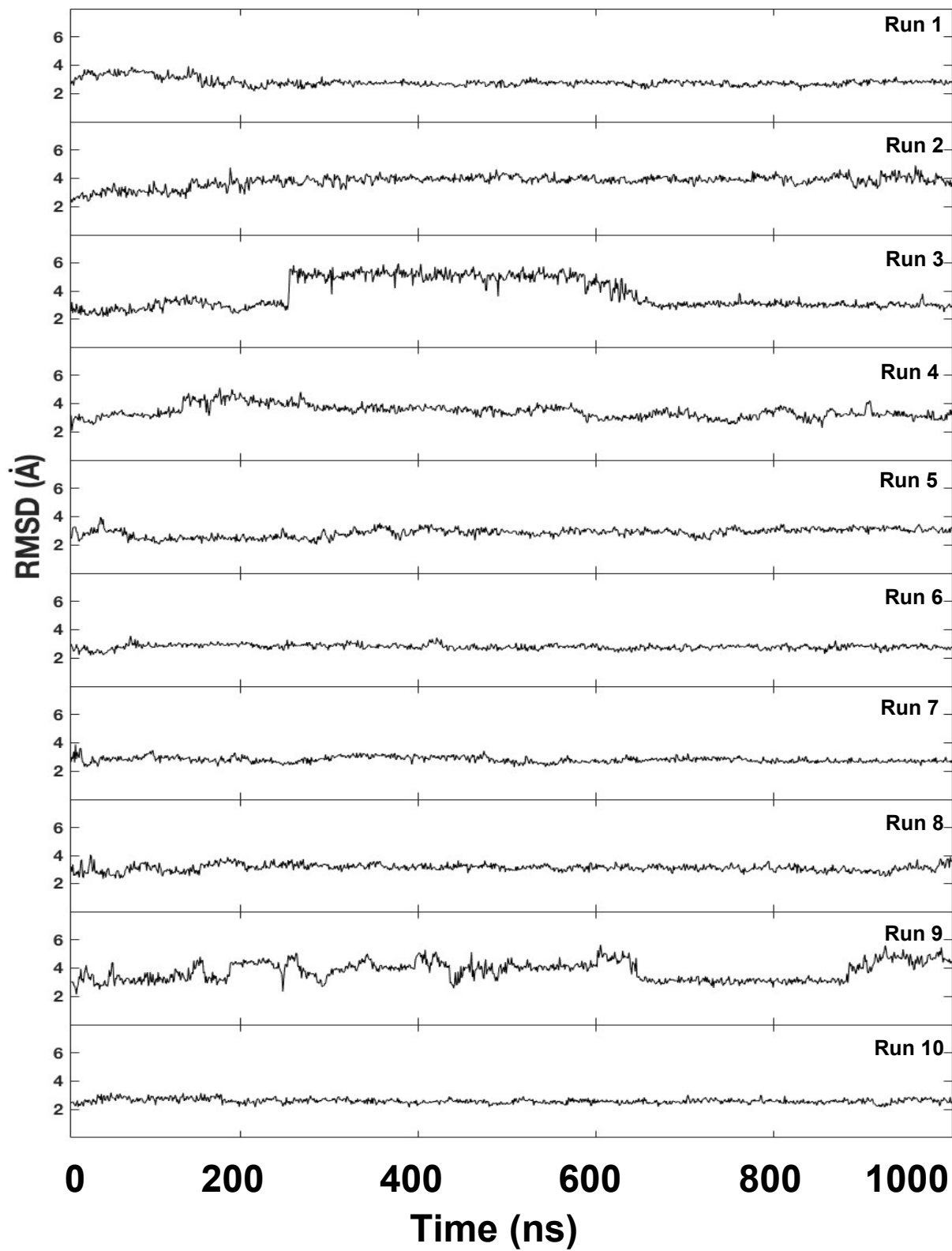


Figure S7. RMSD of hybrid DNA quadruplex system and RHPS4 of each trajectory

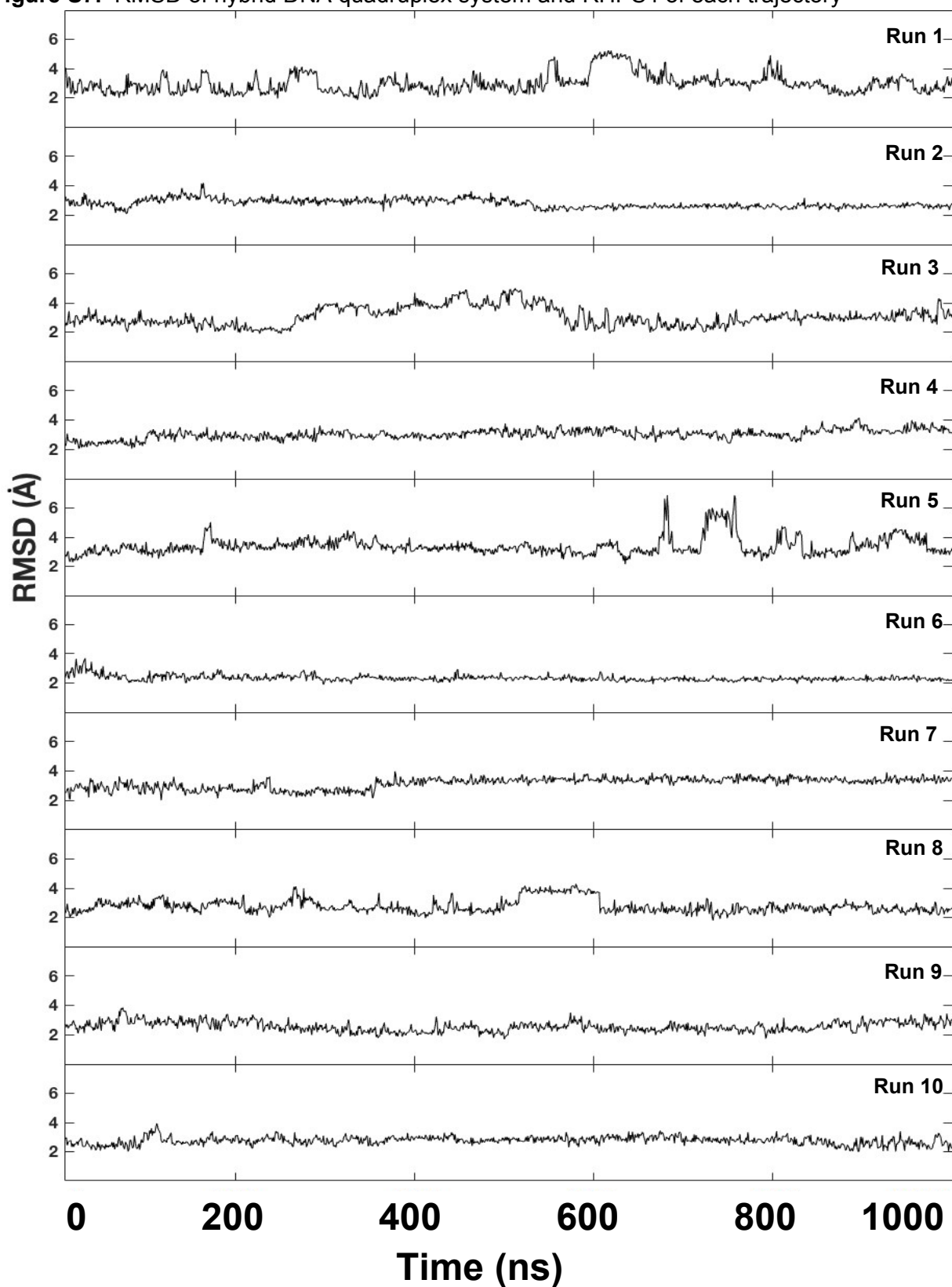


Figure S8. Contact number between duplex DNA system and RHPS4 of each trajectory

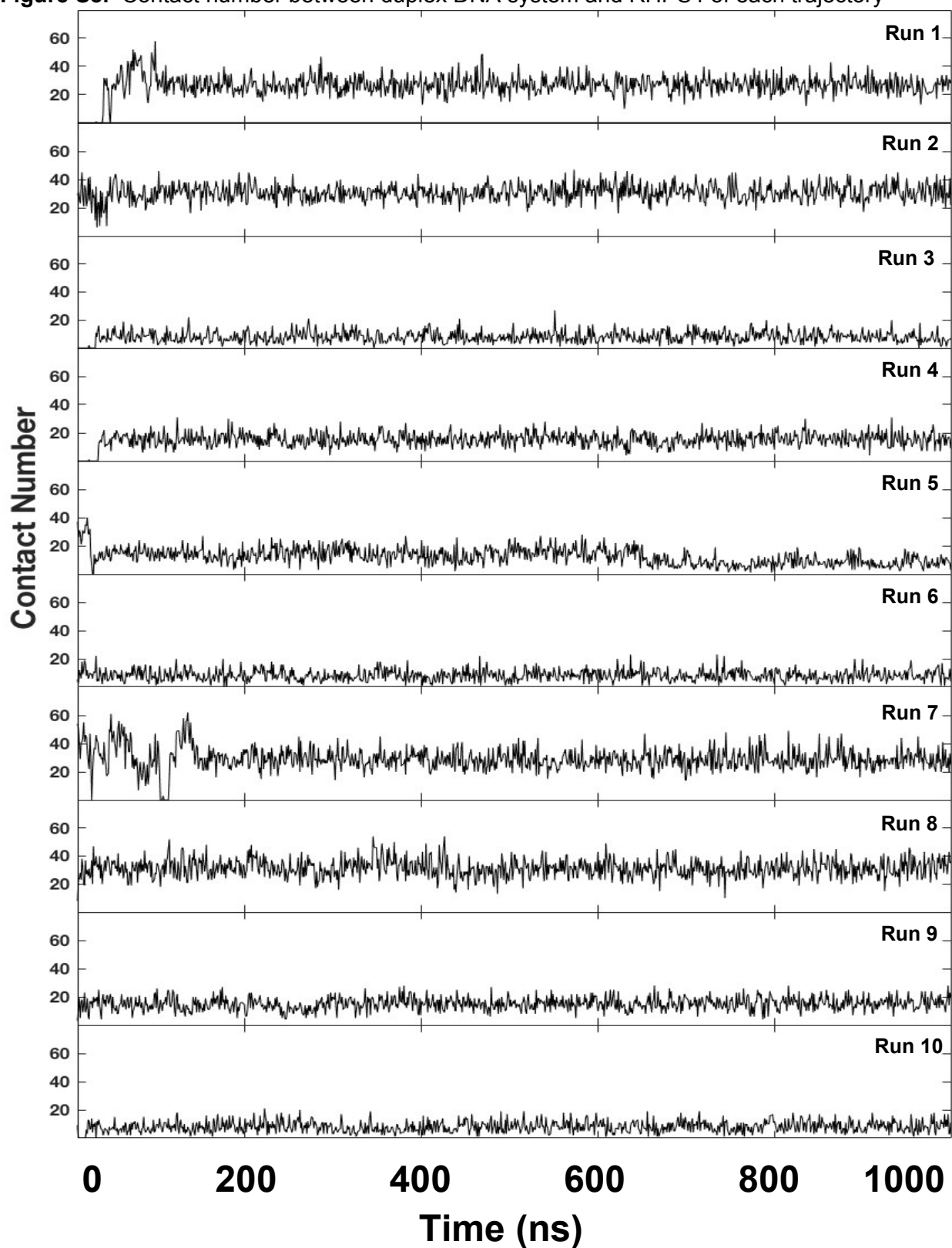


Figure S9. Contact number between parallel DNA quadruplex system and RHPS4 of each trajectory

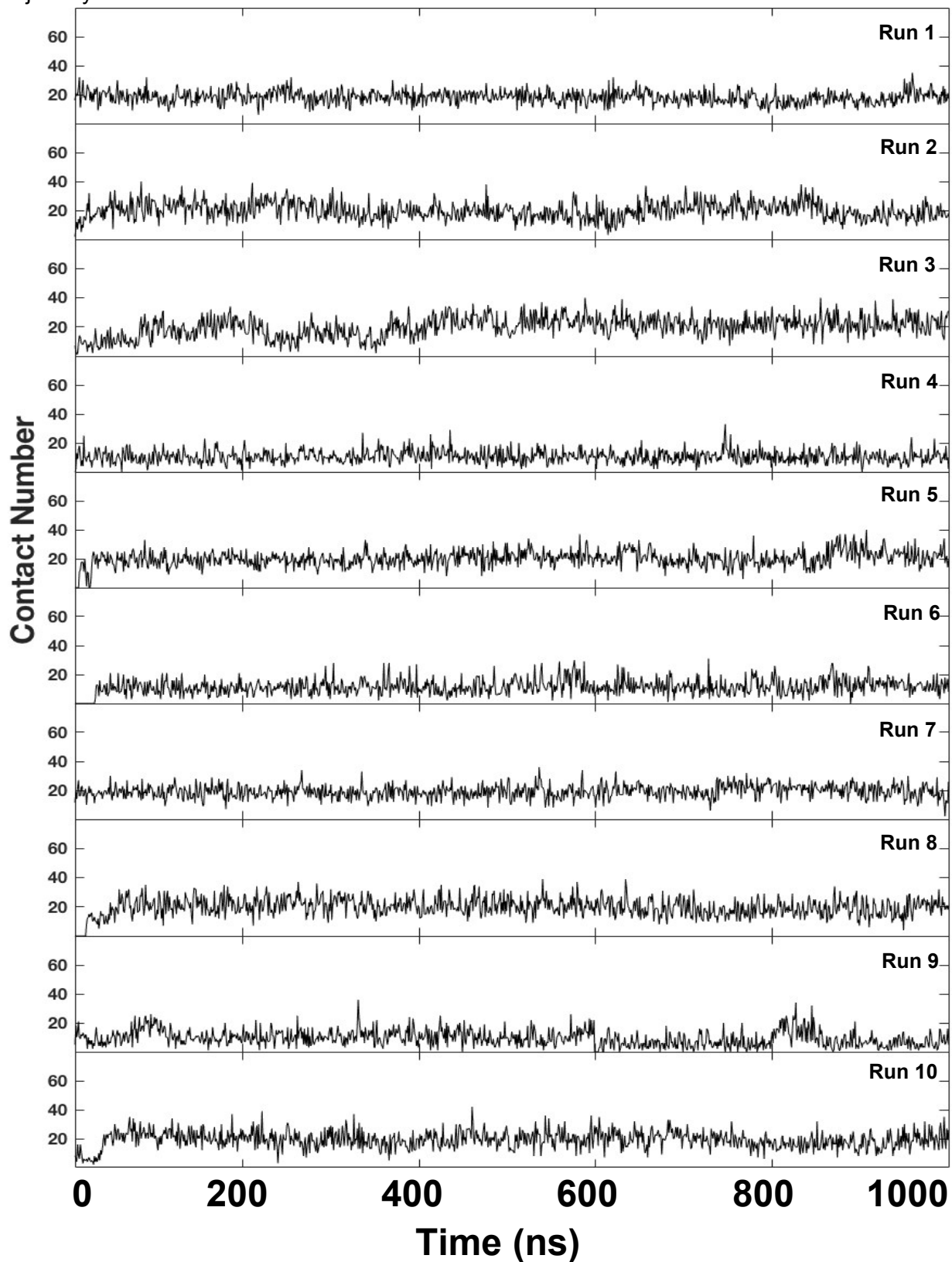


Figure S10. Contact number between antiparallel DNA quadruplex system and RHPS4 of each trajectory

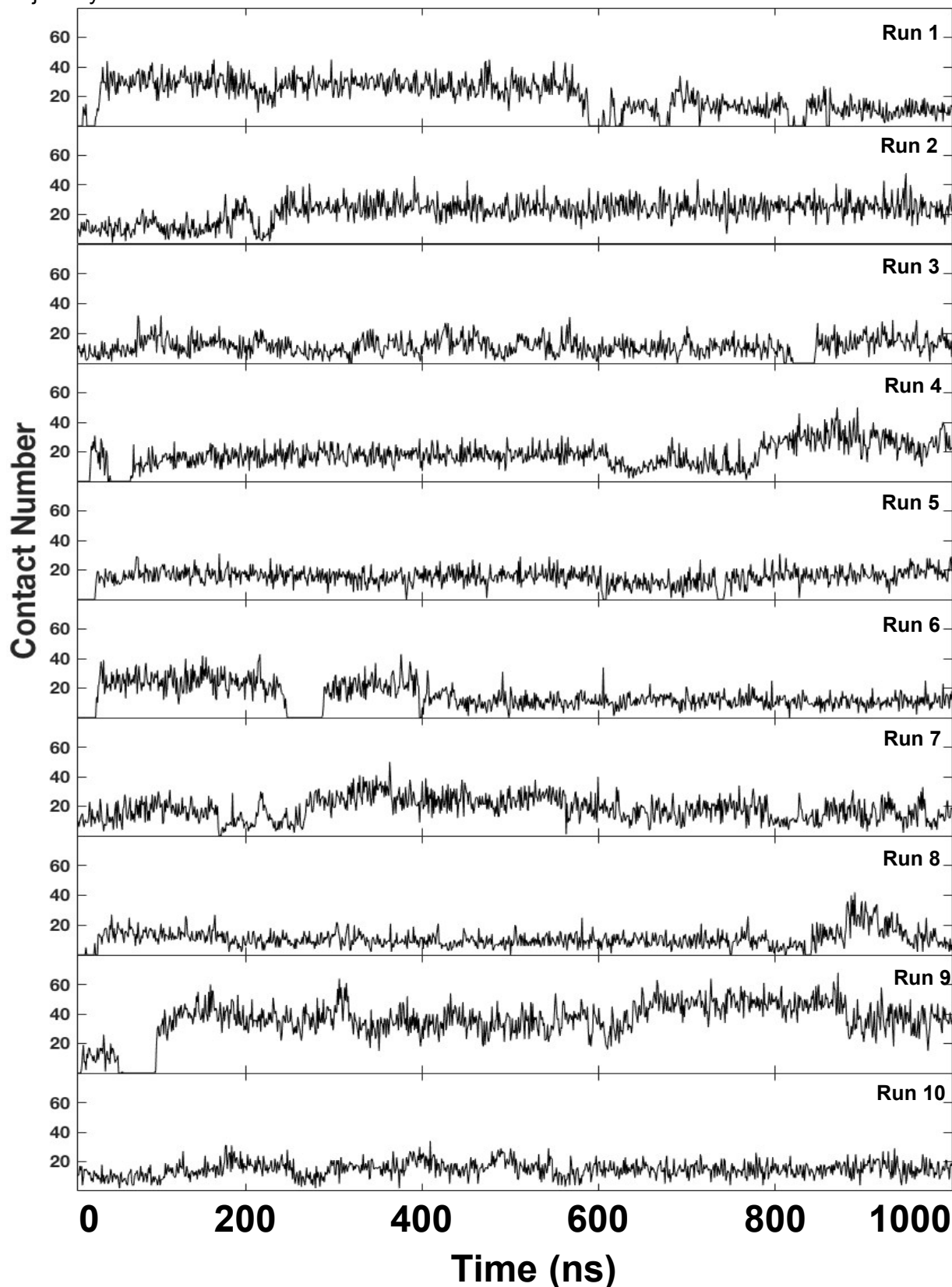


Figure S11. Contact number between hybrid DNA quadruplex system and RHPS4 of each trajectory

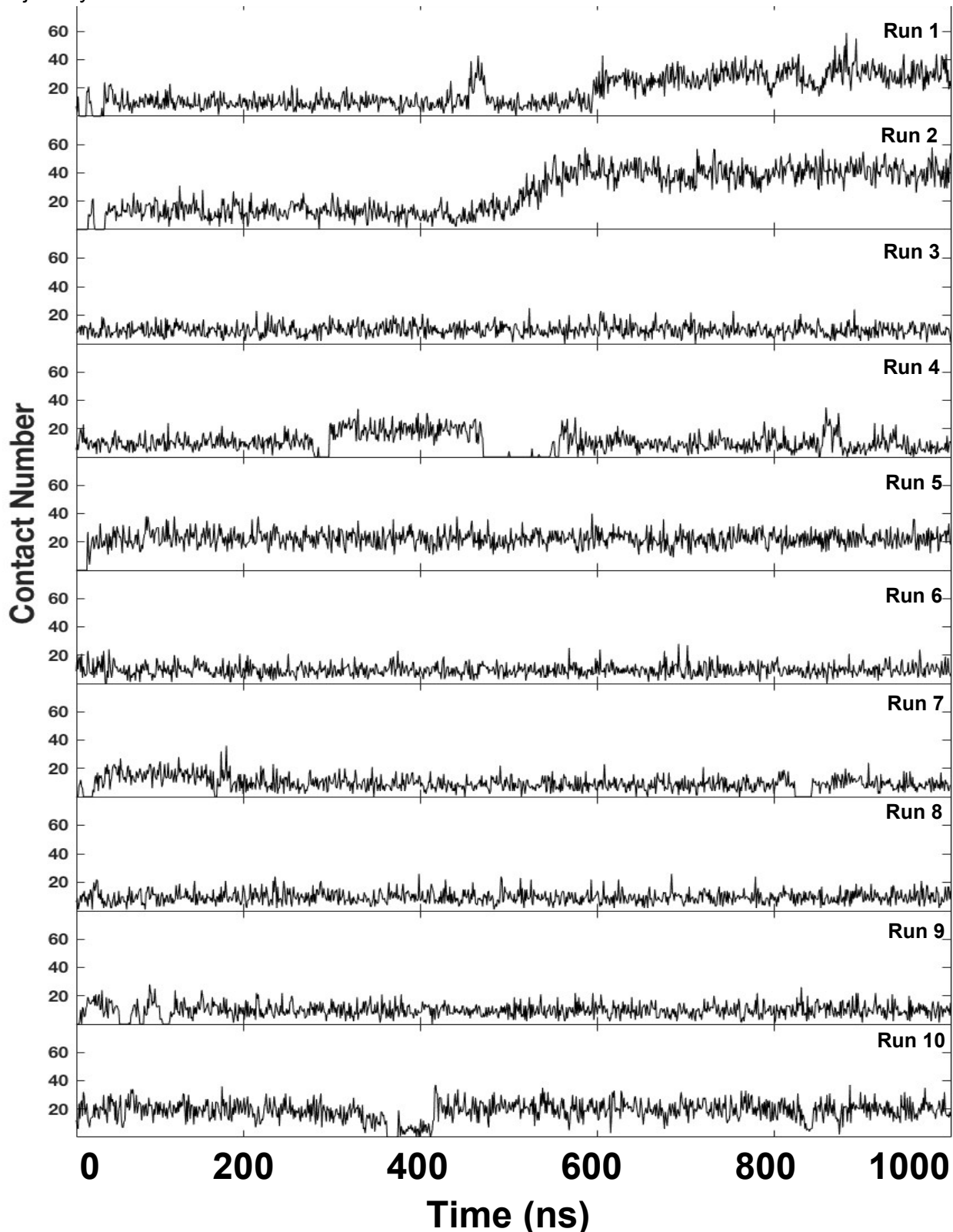
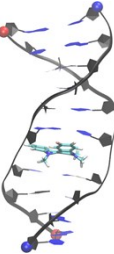
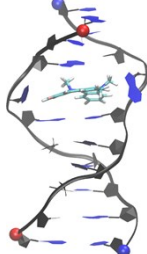
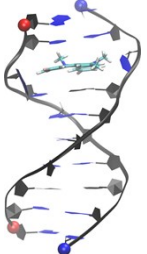
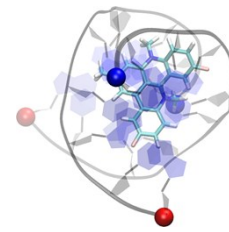
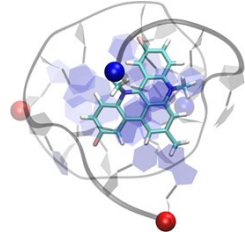
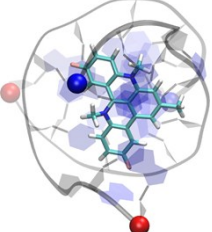
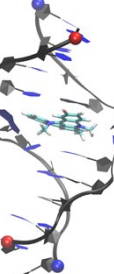
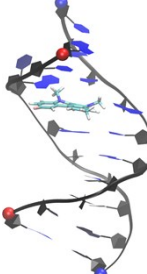
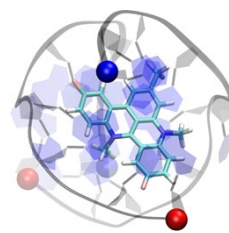
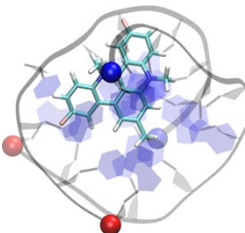
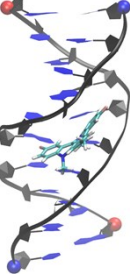
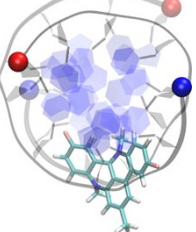


Figure S12. Representative structures of the most populated complex structure families (population $\geq 1\%$) of human telomeric duplex DNA from the clustering analysis of the combined binding trajectories. 5' and 3' are indicated by a red and blue ball, respectively.

Binding Mode	Intercalation Binding		
Cluster ID	A1	A2	A3
Representative Structure (Front View)			
Representative Structure (Top View)			
Population	23%	22%	20%
Cluster ID	A4	A5	
Representative Structure (Front View)			
Representative Structure (Top View)			
Population	19%	1%	

Binding Mode	Groove Binding
Cluster ID	B1
Representative Structure (Front View)	
Representative Structure (Top View)	
Population	5%

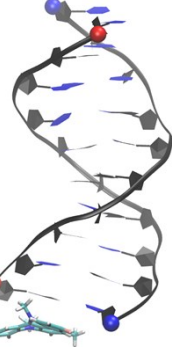
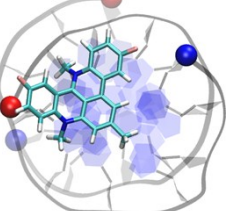
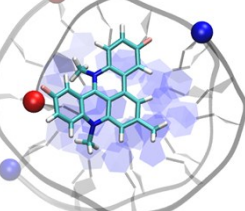
Binding Mode	Bottom-Stacking	Top-Stacking
Cluster ID	D1	C1
Representative Structure (Front View)		
Representative Structure (Top View)		
Population	5%	3%

Figure S13. Last snapshot of ten parallel G-quadruplex-RHPS4 simulations. 5', 3' and K⁺ are indicated by a red, blue and yellow ball, respectively.

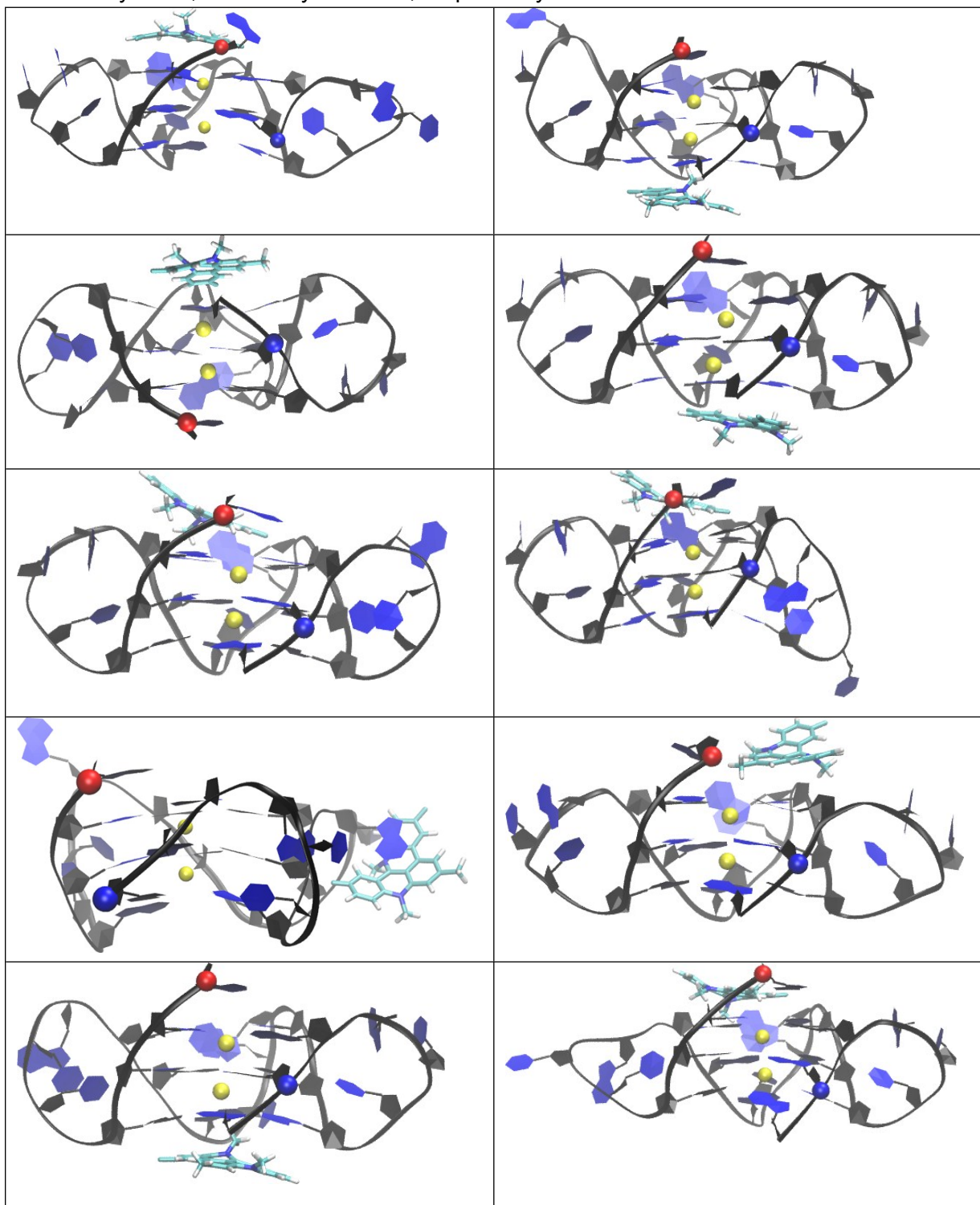
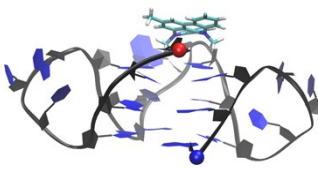
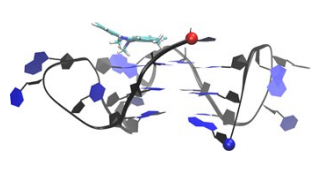
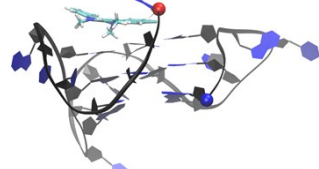
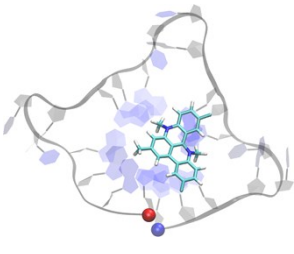
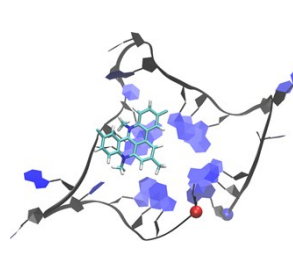
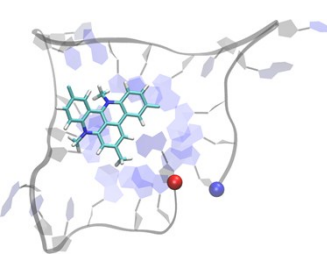
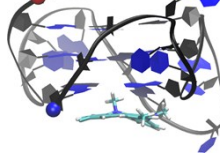
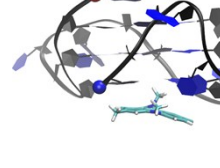
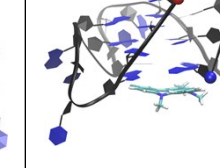
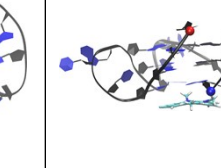
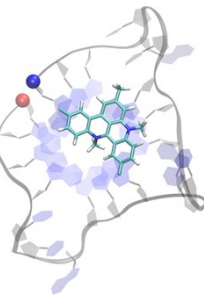
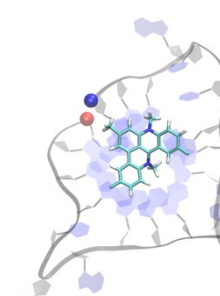
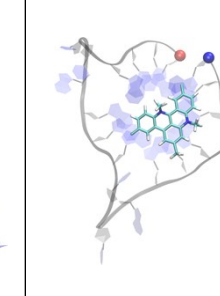
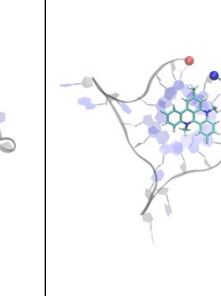


Figure S14. Representative structures of the most populated complex structure families (population $\geq 1\%$) of human telomeric parallel quadruplex DNA from the clustering analysis of the combined binding trajectories. 5' and 3' are indicated by a red and blue ball, respectively.

Binding Mode	Top-Stacking		
Cluster ID	A1	A2	A3
Representative Structure (Front View)			
Representative Structure (Top View)			
Population	52%	17%	4%

Binding Mode	Bottom-Stacking			
Cluster ID	B1	B2	B3	B4
Representative Structure (Front View)				
Representative Structure (Top View)				

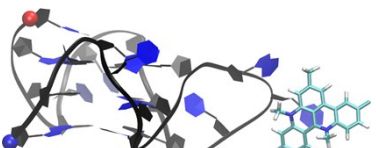
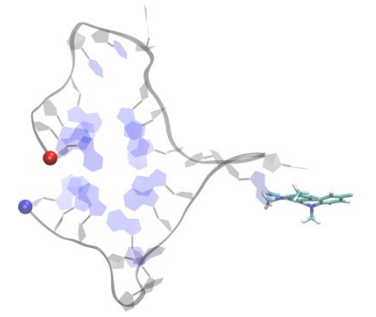
Population	13%	5%	4%	4%
Binding Mode	Side-Loop Binding			
Cluster ID	C1			
Representative Structure (Front View)				
Representative Structure (Top View)				
Population	5%			

Figure S15. Last snapshot of ten anti-parallel G-quadruplex-RHPS4 simulations. 5', 3' and Na⁺ are indicated by a red, blue and yellow ball, respectively.

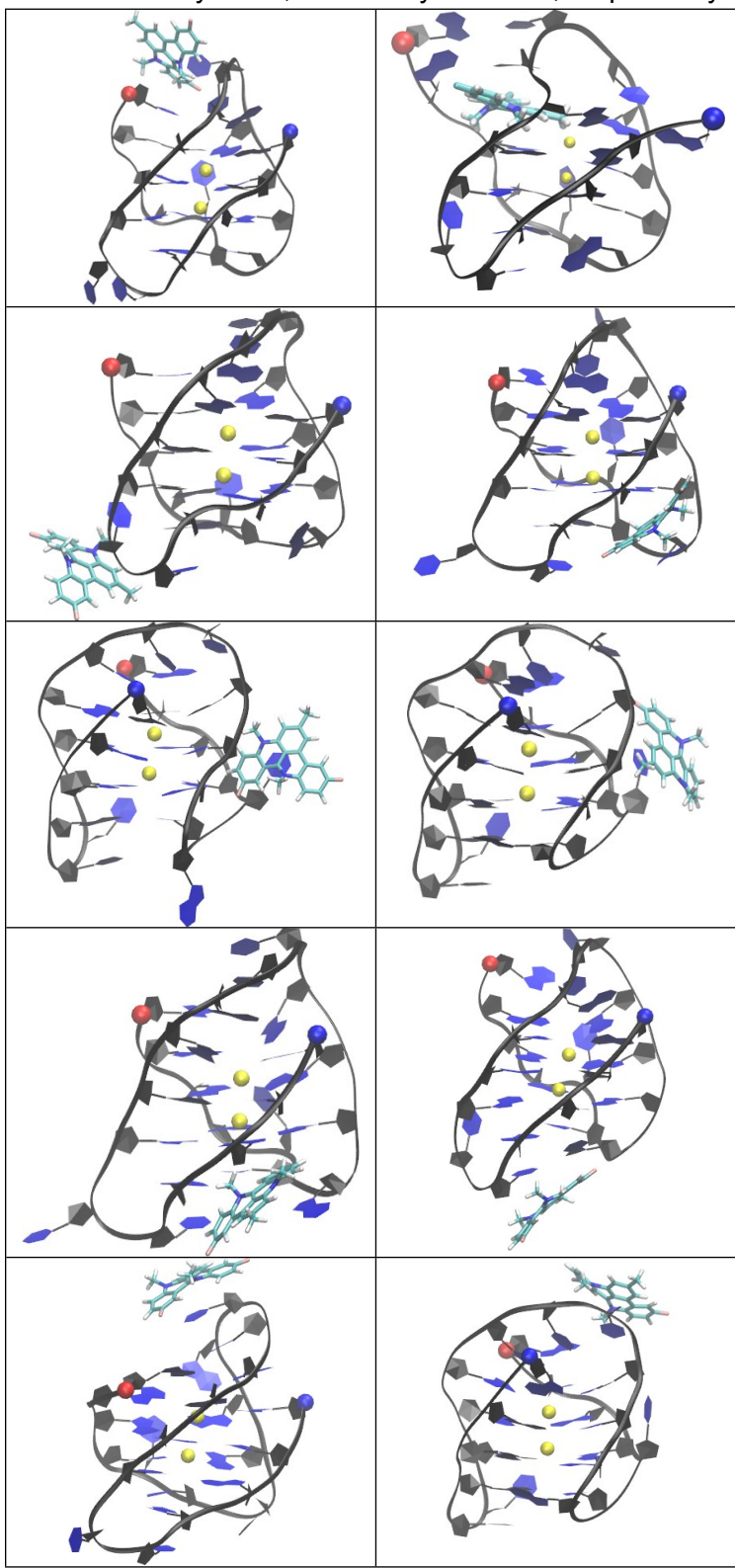
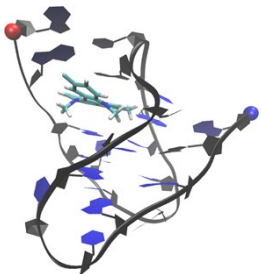
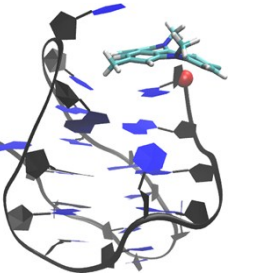
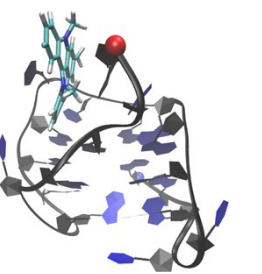
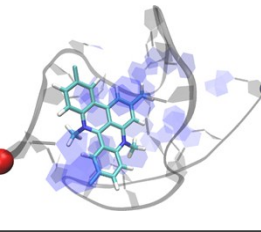
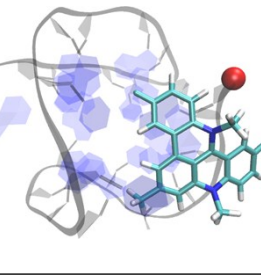
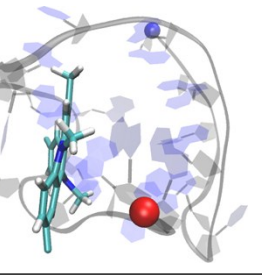
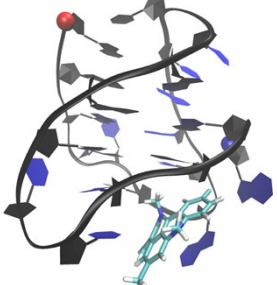
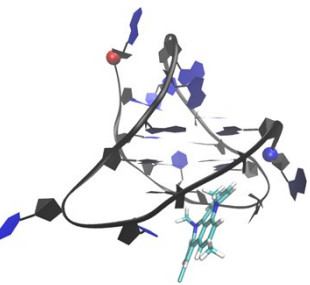
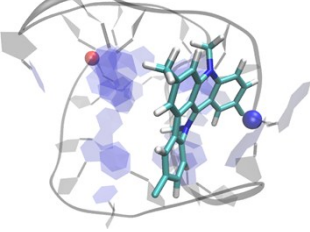
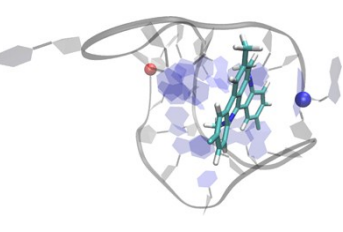


Figure S16. Representative structures of the most populated complex structure families (population $\geq 1\%$) of human telomeric antiparallel quadruplex DNA from the clustering analysis of the combined binding trajectories. 5' and 3' are indicated by a red and blue ball, respectively.

Binding Mode	Top Intercalation/Insertion		
Cluster ID	A1	A2	A3
Representative Structure (Front View)			
Representative Structure (Top View)			
Population	19%	17%	11%

Binding Mode	Bottom Insertion	
Cluster ID	B1	B2
Representative Structure (Front View)		
Representative Structure (Top View)		
Population	35%	6%

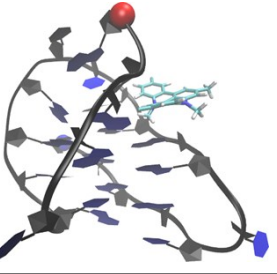
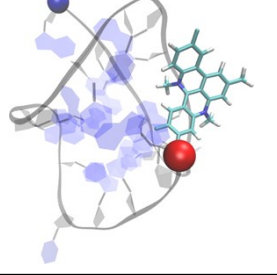
Binding Mode	Side-Groove Binding
Cluster ID	C1
Representative Structure (Front View)	
Representative Structure (Top View)	
Population	5%

Figure S17. Last snapshot of ten hybrid G-quadruplex-RHPS4 simulations. 5', 3' and K⁺ are indicated by a red, blue and yellow ball, respectively.

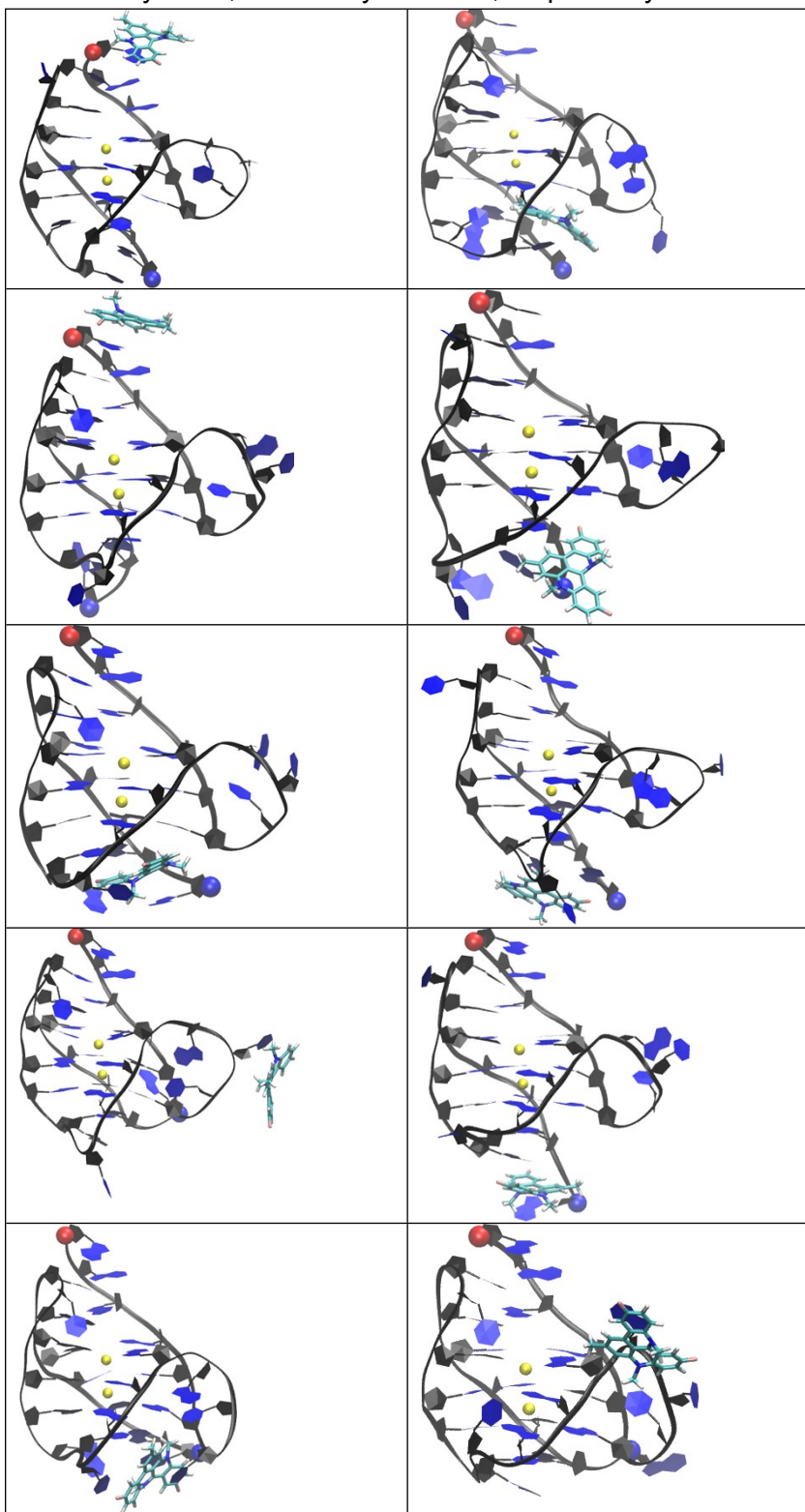
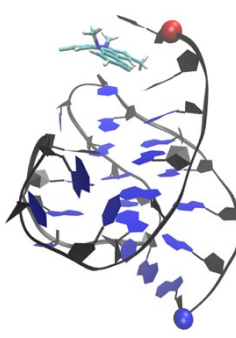
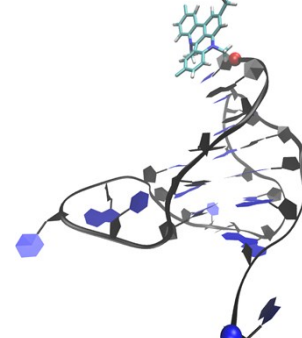
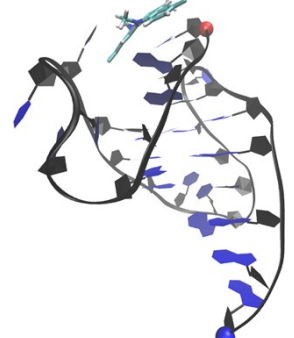
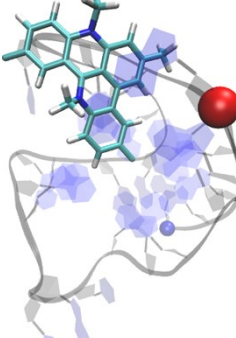
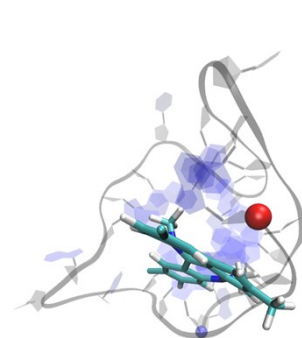
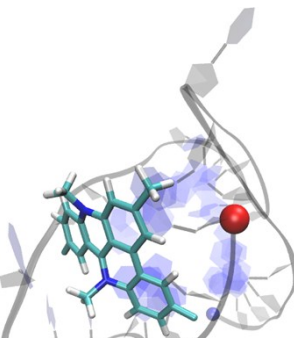
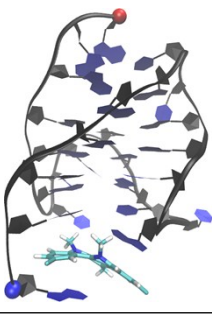
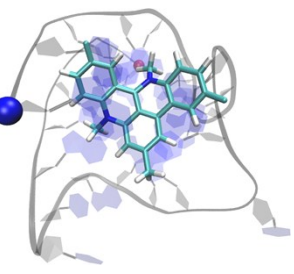


Figure S18. Representative structures of the most populated complex structure families (population $\geq 1\%$) of human telomeric hybrid quadruplex DNA from the clustering analysis of the combined binding trajectories. 5' and 3' are indicated by a red and blue ball, respectively.

Binding Mode	Top-Stacking		
Cluster ID	A1	A2	A3
Representative Structure (Front View)			
Representative Structure (Top View)			
Population	62%	4%	2%

Binding Mode	Bottom-Stacking
Cluster ID	B1
Representative Structure (Front View)	
Representative Structure (Top View)	
Population	16%

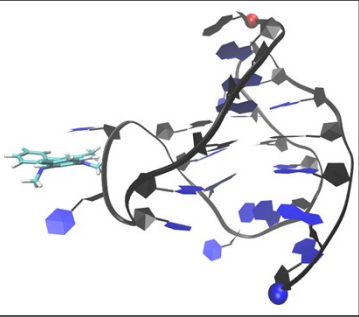
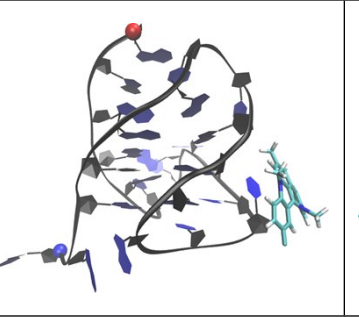
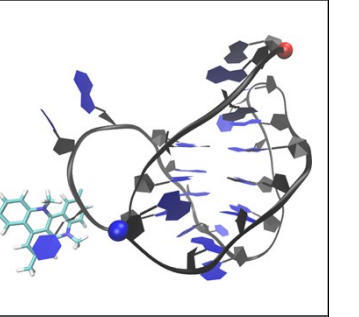
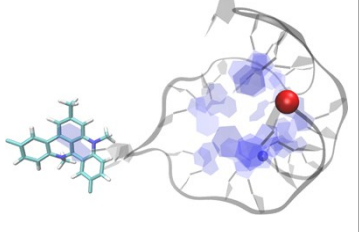
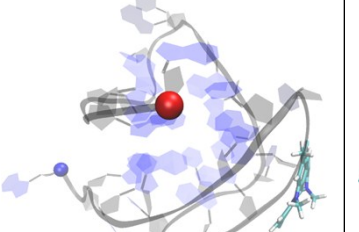
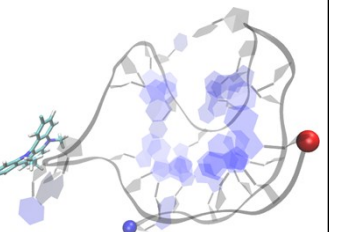
Binding Mode	Side-Loop Binding		
Cluster ID	C1	C2	C3
Representative Structure (Front View)			
Representative Structure (Top View)			
Population	8%	3%	2%

Figure S19. A trajectory of RHPS4 intercalating to human telomeric duplex DNA with a broken base pair. The order parameters include hydrogen bonds in first (red), second (blue) and third (yellow) of duplex base paring layer (H-Bond), center-to-center distance (R), the drug-base dihedral angle, ligand RMSD and MM-GBSA binding energy (ΔE). 5' and 3' of the DNA chain are indicated by a red and blue ball, respectively.

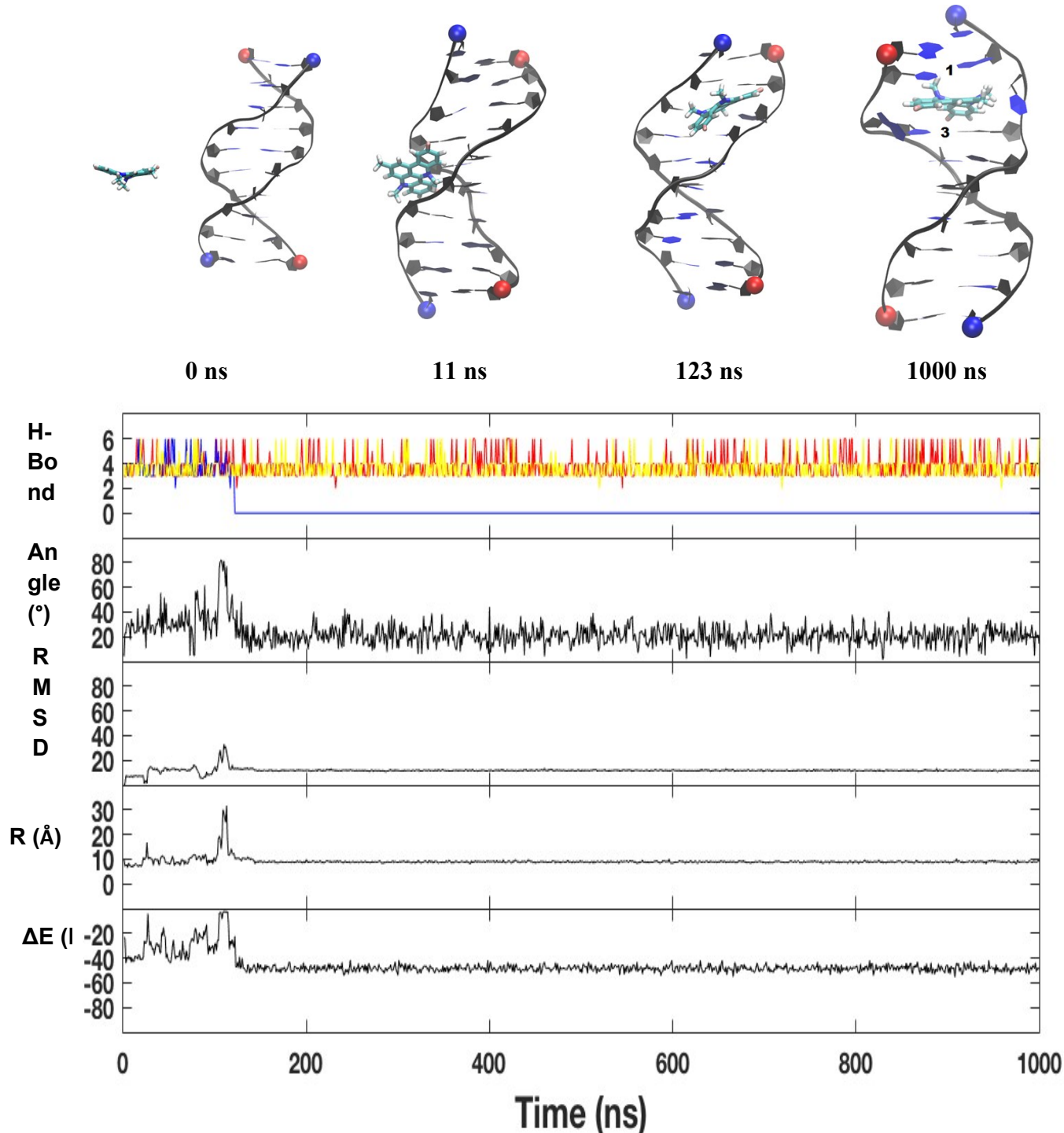


Figure S20. A trajectory of RHPS4 intercalating to human telomeric duplex DNA with a broken base pair. The order parameters include hydrogen bonds in first (red), second (blue) and third (yellow) of duplex base paring layer (H-Bond), center-to-center distance (R), the drug-base dihedral angle, ligand RMSD and MM-GBSA binding energy (ΔE). 5' and 3' of the DNA chain are indicated by a red and blue ball, respectively.

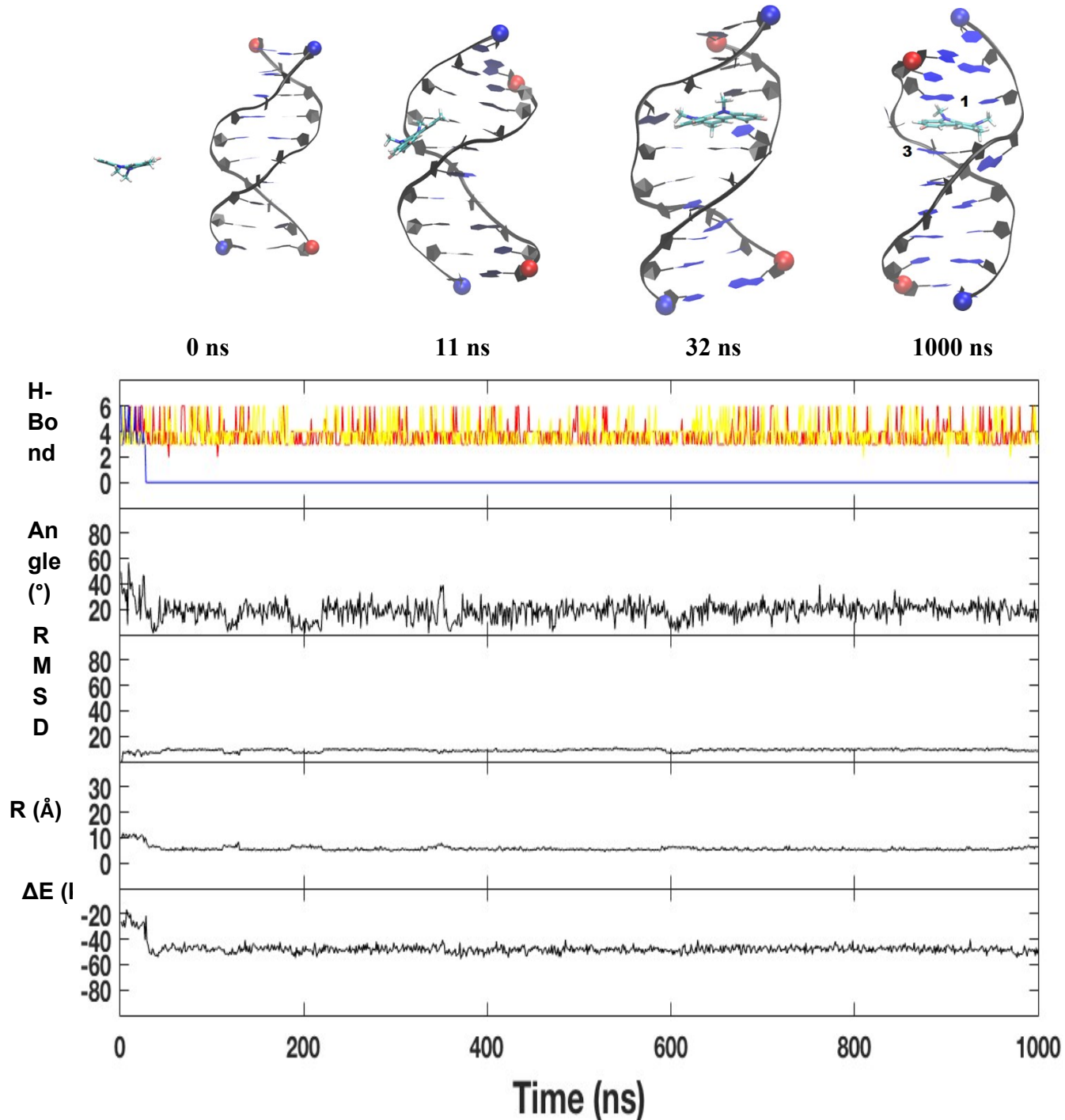


Figure S21. A representative trajectory of RHPS4 binding to the top of human telomeric parallel quadruplex DNA. The order parameter include hydrogen bonds present in first (red), second (blue) and third (yellow) of G-tetrad layer of quadruplex (H-Bond), center-to-center distance (R), the drug-base dihedral angle, ligand RMSD and MM-GBSA binding energy (ΔE). 5' and 3' of the DNA chain are indicated by a red and blue ball, respectively.

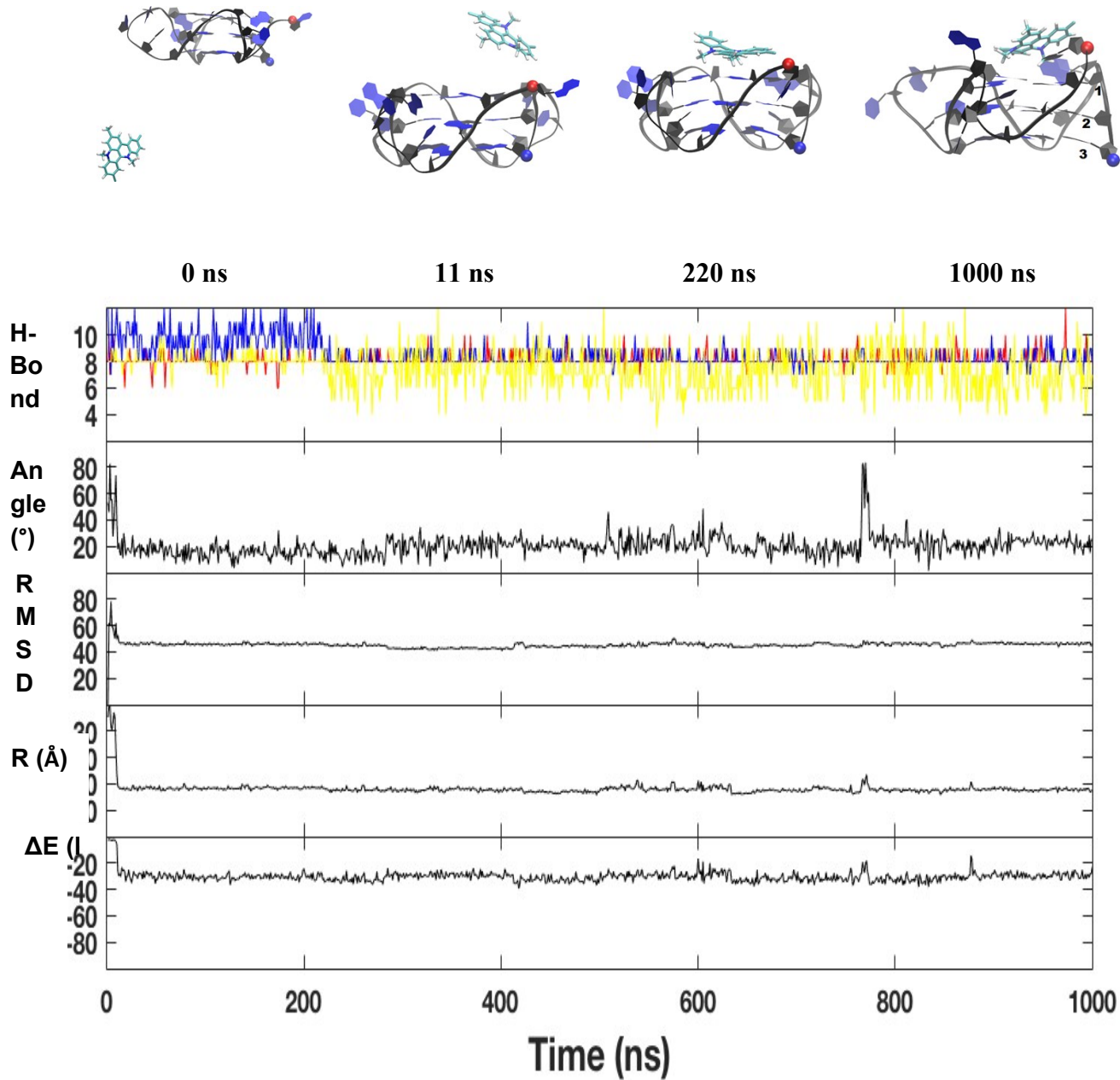


Figure S22. A representative trajectory of RHPS4 binding to the side loop of human telomeric parallel DNA quadruplex. The order parameter include hydrogen bonds present in first (red), second (blue) and third (yellow) of G-tetrad layer of quadruplex (H-Bond), center-to-center distance (R), the drug-base dihedral angle, ligand RMSD and MM-GBSA binding energy (ΔE). 5' and 3' of the DNA chain are indicated by a red and blue ball, respectively.

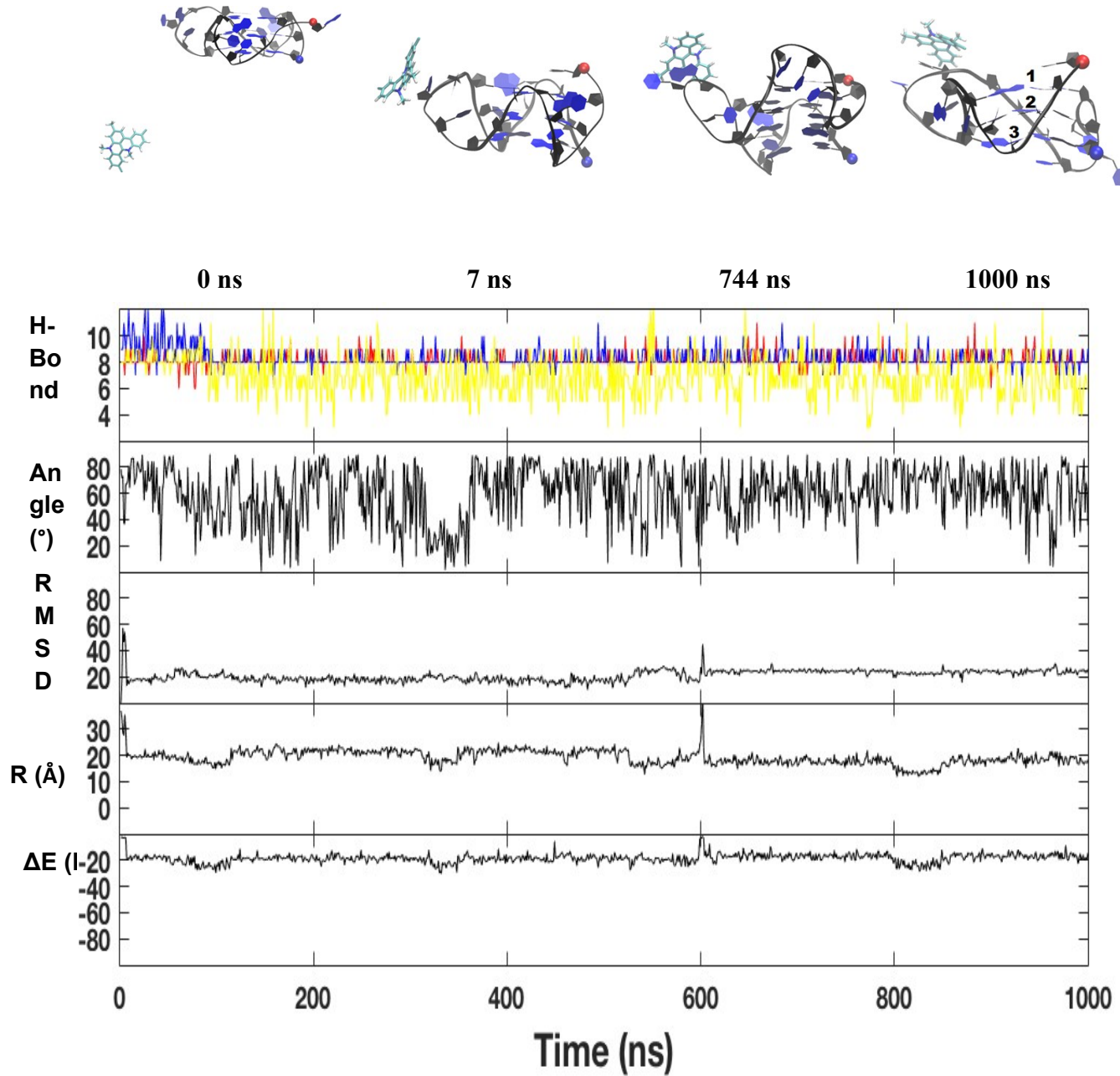


Figure S23. A representative trajectory of RHPS4 binding to the bottom of human telomeric antiparallel DNA quadruplex. The order parameter include hydrogen bonds present in first (red), second (blue) and third (yellow) of G-tetrad layer of quadruplex (H-Bond), center-to-center distance (R), the drug-base dihedral angle, ligand RMSD and MM-GBSA binding energy (ΔE). 5' and 3' of the DNA chain are indicated by a red and blue ball, respectively.

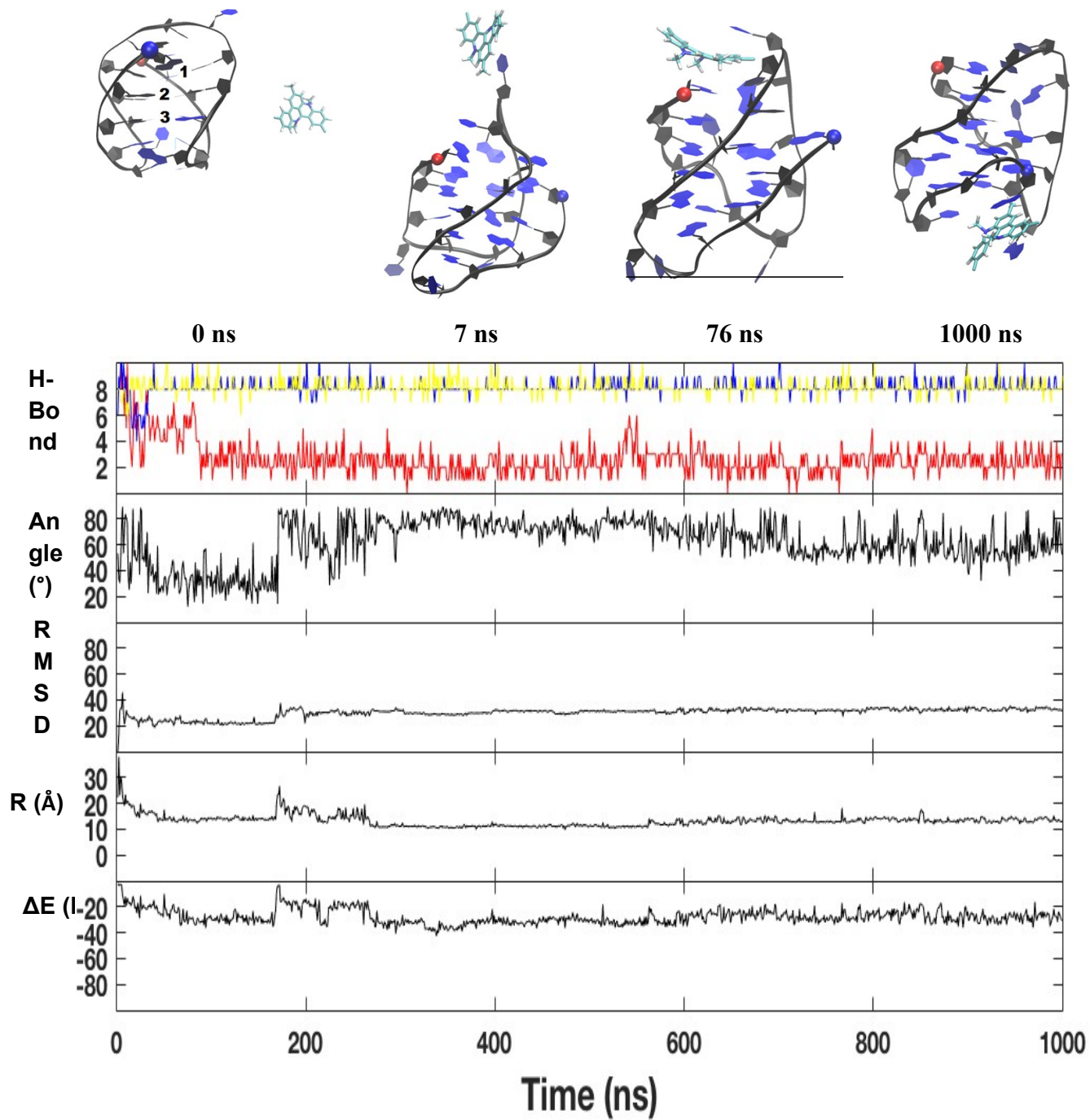


Figure S24. A representative trajectory of RHPS4 binding to the bottom of human telomeric antiparallel DNA quadruplex. The order parameter include hydrogen bonds present in first (red), second (blue) and third (yellow) of G-tetrad layer of quadruplex (H-Bond), center-to-center distance (R), the drug-base dihedral angle, ligand RMSD and MM-GBSA binding energy (ΔE). 5' and 3' of the DNA chain are indicated by a red and blue ball, respectively.

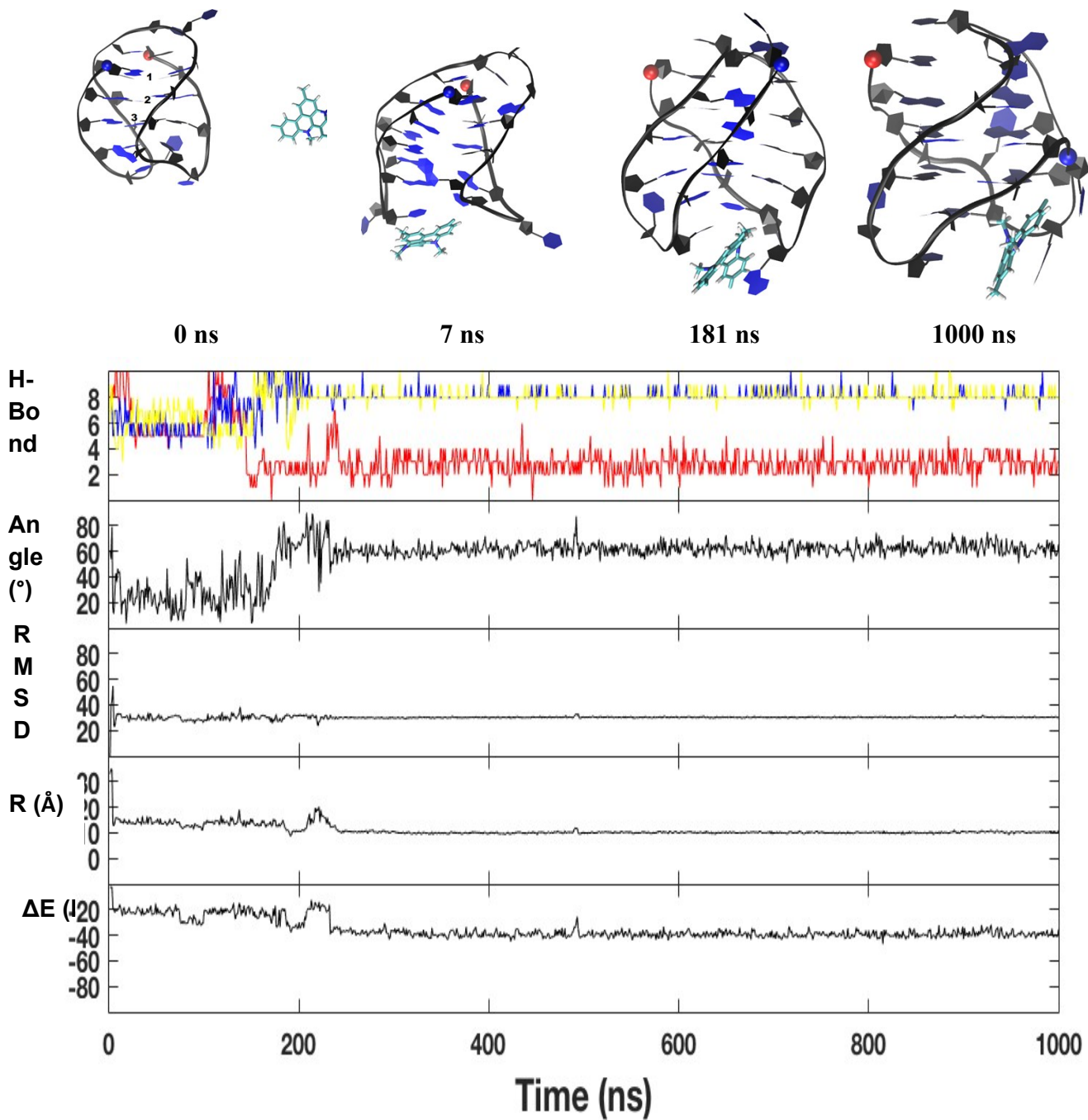


Figure S25. A representative trajectory of RHPS4 binding to the side loop of human telomeric antiparallel DNA quadruplex. The order parameter include hydrogen bonds present in first (red), second (blue) and third (yellow) of G-tetrad layer of quadruplex (H-Bond), center-to-center distance (R), the drug-base dihedral angle, ligand RMSD and MM-GBSA binding energy (ΔE). 5' and 3' of the DNA chain are indicated by a red and blue ball, respectively.

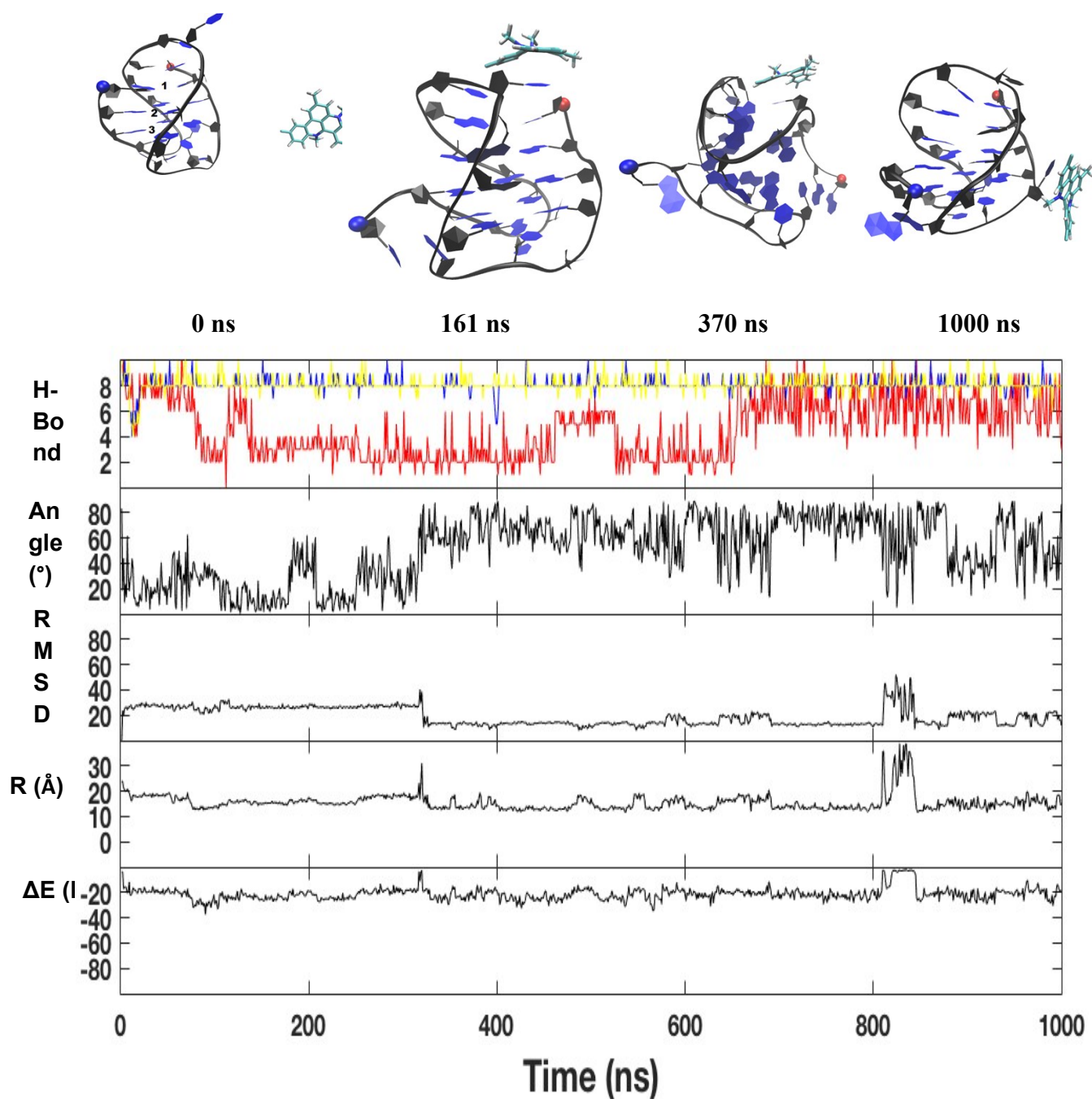


Figure S26. A representative trajectory of RHPS4 stacking to the top of human telomeric hybrid DNA quadruplex. The order parameter include hydrogen bonds present in first (red), second (blue) and third (yellow) of G-tetrad layer of quadruplex (H-Bond), center-to-center distance (R), the drug-base dihedral angle, ligand RMSD and MM-GBSA binding energy (ΔE). 5' and 3' of the DNA chain are indicated by a red and blue ball, respectively.

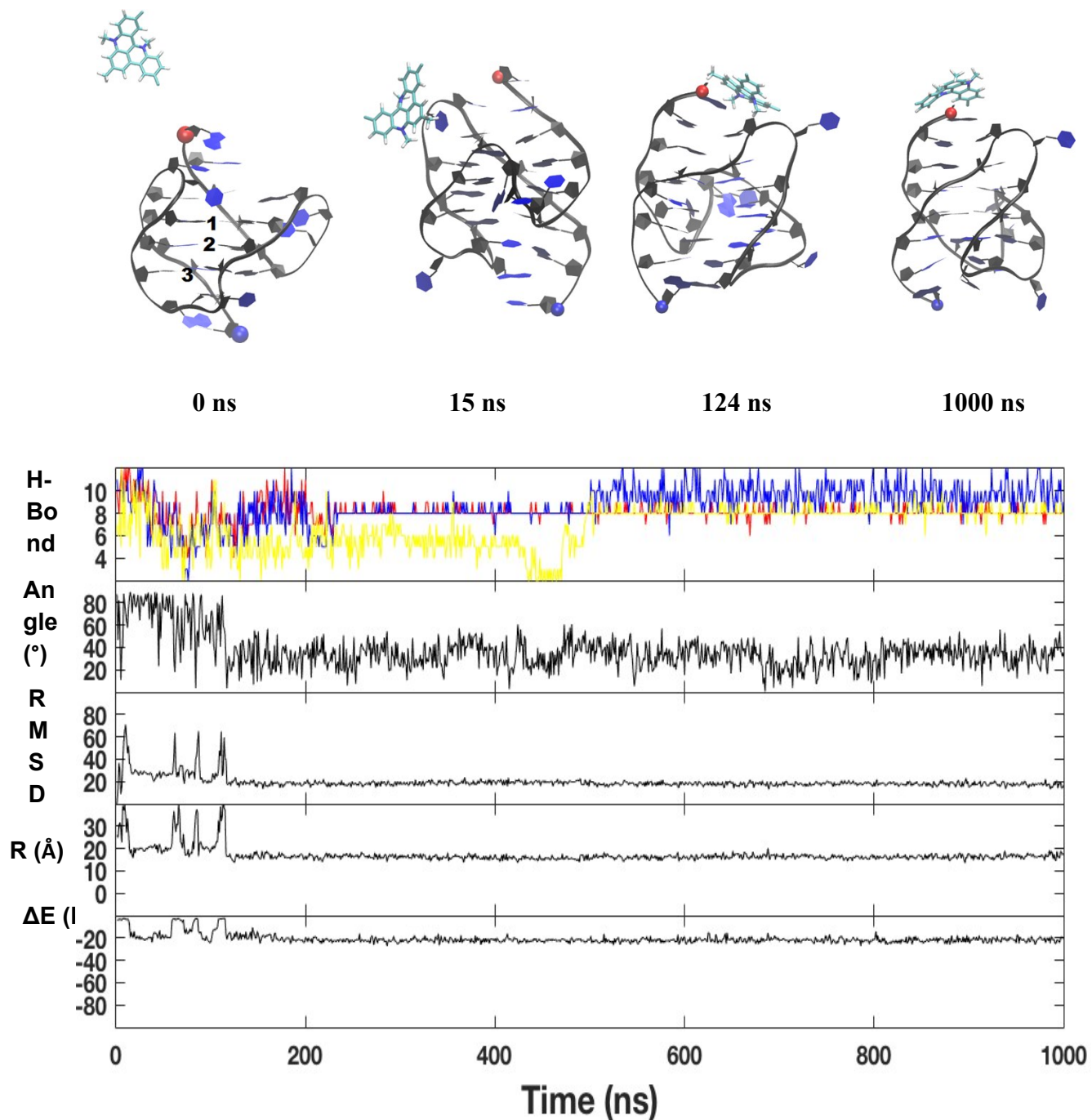


Figure S27. A representative trajectory of RHPS4 binding to the side-groove of human telomeric hybrid DNA quadruplex. Center-to-center distance (R), the drug-base dihedral angle, ligand RMSD and MM-GBSA binding energy (ΔE). 5' and 3' of the DNA chain are indicated by a red and blue ball, respectively.

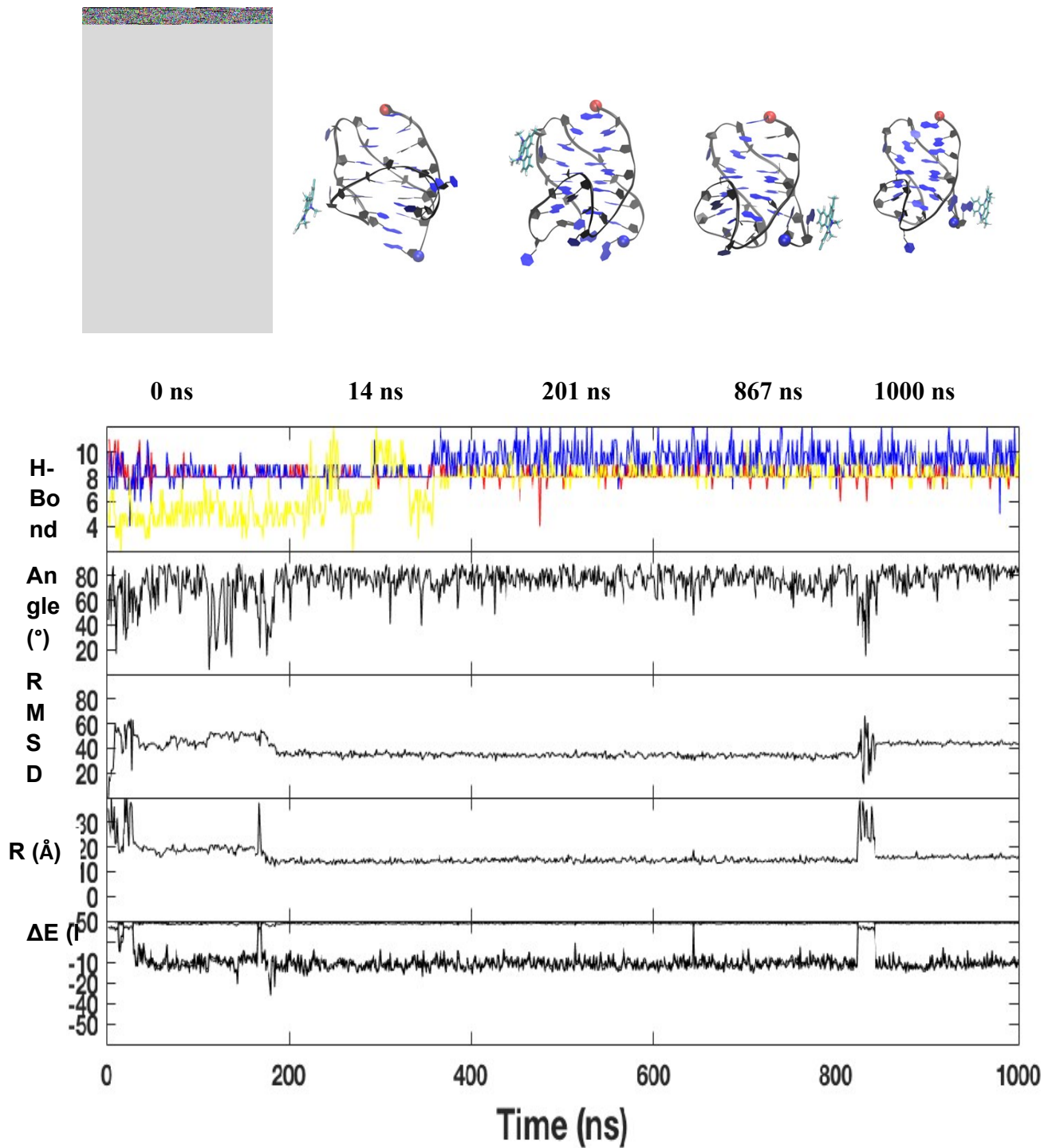


Figure S28. AMBER GAFF2 force field of RHPS4 (+1) in Mol2 format.

```
@<TRIPOS>MOLECULE
LG1
 43  47   1   0   1
SMALL
USER_CHARGES
@<TRIPOS>ATOM
 1 C05    -4.633283  -0.879556  -0.410733 C    1 LG1    -0.039648
 2 H09    -5.685850  -0.984618  -0.594163 H    1 LG1     0.169889
 3 C06    -4.088818   0.338063  -0.120959 C    1 LG1    -0.069123
 4 H10    -4.730669   1.193743  -0.103335 H    1 LG1     0.107580
 5 C01    -2.700480   0.479750   0.085709 C    1 LG1    -0.012257
 6 N14    -2.142871   1.723490   0.280836 N    1 LG1    -0.003253
 7 C13    -0.798672   1.909236   0.094583 C    1 LG1    -0.002912
 8 C18    -0.252244   3.188724  -0.025402 C    1 LG1    -0.058652
 9 H26    -0.890076   4.047234  -0.054356 H    1 LG1     0.098625
10 C17    1.110085   3.370543  -0.145221 C    1 LG1    -0.055059
11 C16    1.970963   2.267576  -0.134051 C    1 LG1    -0.058247
12 H28    3.025862   2.443512  -0.200435 H    1 LG1     0.116197
13 C15    1.475559   0.991668  -0.033717 C    1 LG1    -0.019249
14 C19    2.317536  -0.205373  -0.032496 C    1 LG1    -0.025508
15 C20    3.688499  -0.152691  -0.309714 C    1 LG1    -0.028871
16 H29    4.175684   0.765505  -0.566568 H    1 LG1     0.140390
17 C21    4.436576  -1.293739  -0.268996 C    1 LG1    -0.003493
18 F30    5.727948  -1.230270  -0.533712 F    1 LG1    -0.084337
19 C22    3.873787  -2.523126  0.035187 C    1 LG1    -0.042024
20 H31    4.487805  -3.403137  0.046013 H    1 LG1     0.153671
21 C23    2.528662  -2.589890  0.299952 C    1 LG1    -0.072281
22 H32    2.097756  -3.547475  0.508451 H    1 LG1     0.103667
23 C24    1.738465  -1.435703  0.268823 C    1 LG1    -0.019030
24 NP5    0.348207  -1.533479  0.506008 N    1 LG1     0.023646
25 C11    -0.462110  -0.506249  0.228254 C    1 LG1     0.073884
26 C02    -1.890072  -0.663637  0.044008 C    1 LG1     0.011322
27 C03    -2.470218  -1.904999  -0.308057 C    1 LG1    -0.019154
28 H07    -1.872254  -2.778425  -0.457763 H    1 LG1     0.117318
29 C04    -3.804487  -1.996499  -0.519540 C    1 LG1    -0.012023
30 F08    -4.340081  -3.155268  -0.860380 F    1 LG1    -0.088658
31 C12    0.071532   0.791445   0.064029 C    1 LG1     0.046444
32 C34    -0.110828  -2.699161  1.283618 C    1 LG1    -0.000787
```

33 H35	0.594764	-2.858288	2.084924 H	1 LG1	0.070118
34 H36	-1.072647	-2.489904	1.716164 H	1 LG1	0.070118
35 H37	-0.171204	-3.592102	0.678483 H	1 LG1	0.070118
36 C27	1.688665	4.754603	-0.292167 C	1 LG1	-0.022544
37 H38	2.401816	4.951947	0.501035 H	1 LG1	0.053165
38 H39	0.921182	5.516146	-0.256793 H	1 LG1	0.053165
39 H40	2.214743	4.844969	-1.236584 H	1 LG1	0.053165
40 C33	-2.991755	2.859435	0.646868 C	1 LG1	-0.008669
41 H41	-3.357953	3.385684	-0.226369 H	1 LG1	0.071099
42 H42	-3.823513	2.506508	1.233227 H	1 LG1	0.071099
43 H43	-2.427791	3.535943	1.267122 H	1 LG1	0.071099

@<TRIPOS>BOND

1	1	2 1
2	1	3 1
3	1	29 1
4	3	4 1
5	3	5 1
6	5	6 1
7	5	26 1
8	6	7 1
9	6	40 1
10	7	8 1
11	7	31 1
12	8	9 1
13	8	10 1
14	10	11 1
15	10	36 1
16	11	12 1
17	11	13 1
18	13	14 1
19	13	31 1
20	14	15 1
21	14	23 1
22	15	16 1
23	15	17 1
24	17	18 1
25	17	19 1
26	19	20 1
27	19	21 1
28	21	22 1

29 21 23 1
30 23 24 1
31 24 25 1
32 24 32 1
33 25 26 1
34 25 31 1
35 26 27 1
36 27 28 1
37 27 29 1
38 29 30 1
39 32 33 1
40 32 34 1
41 32 35 1
42 36 37 1
43 36 38 1
44 36 39 1
45 40 41 1
46 40 42 1
47 40 43 1

@<TRIPOS>SUBSTRUCTURE

1 LG1 1 0